ChemPubSoc Europe

DOI: 10.1002/cmdc.201300469

Synthesis, Antimalarial Properties, and SAR Studies of Alkoxyurea-Based HDAC Inhibitors

Finn K. Hansen,[a] Tina S. Skinner-Adams,[b] Sandra Duffy,[b] Linda Marek,[a] Subathdrage D. M. Sumanadasa,[b] Krystina Kuna,[a] Jana Held,[c] Vicky M. Avery,[b] Katherine T. Andrews,*[b] and Thomas Kurz*[a]

Histone deacetylase (HDAC) inhibitors are an emerging class of potential antimalarial drugs. We investigated the antiplasmodial properties of 16 alkoxyurea-based HDAC inhibitors containing various cap and zinc binding groups (ZBGs). Ten compounds displayed sub-micromolar activity against the 3D7 line of *Plasmodium falciparum*. Structure–activity relationship studies revealed that a hydroxamic acid ZBG is crucial for antiplasmodial activity, and that the introduction of bulky alkyl substituents to cap groups increases potency against asexual blood-stage parasites. We also demonstrate that selected compounds cause hyperacetylation of *P. falciparum* histone H4, indicating inhibition of one or more *Pf*HDACs. To assess the selectivity of alkoxyurea-based HDAC inhibitors for parasite over normal mammalian cells, the cytotoxicity of representative compounds was evaluated against neonatal foreskin fibroblast (NFF) cells. The most active compound, 6-((3-(4-(*tert*-butyl)phenyl)ureido)oxy)-*N*-hydroxyhexanamide (**1e**, *Pf*3D7 IC_{50}: 0.16 μM) was 31-fold more toxic against the asexual blood stages than towards normal mammalian cells. Moreover, a subset of four structurally diverse HDAC inhibitors revealed moderate activity against late-stage (IV–V) gametocytes.

Introduction

Malaria, a parasitic infection caused by *Plasmodium* spp., has been among mankind's deadliest diseases. Over 3.3 billion people living in tropical and subtropical regions were at risk in 2011.[1] Children from sub-Saharan Africa take the heaviest burden, and, despite large investments to develop other interventions such as malaria vaccines,[2,3] it is unlikely that malaria can be controlled effectively without the development of new antimalarial drugs. A major limitation of antimalarial drug treatment is the rapid spread of drug-resistant *P. falciparum* parasites.[4] Alarming signs of emerging resistance to artemisinin derivatives in Southeast Asia are now threatening the widely accepted artemisinin combination therapies (ACTs).[5,6] For instance, a recent study conducted in Cambodia revealed that the percentage of patients who were still parasitemic after three days of treatment with dihydroartemisinin–piperaquine increased from 26% in 2008 to 45% in 2010.[7] Accordingly, to tackle drug resistance, there is an urgent need for new antimalarial drug classes with novel modes of action.

[a] *Dr. F. K. Hansen, L. Marek, K. Kuna, Prof. Dr. T. Kurz[+]*
Institute of Pharmaceutical and Medicinal Chemistry
Heinrich Heine University Düsseldorf, 40225 Düsseldorf (Germany)
E-mail: thomas.kurz@uni-duesseldorf.de

[b] *Dr. T. S. Skinner-Adams, S. Duffy, S. D. M. Sumanadasa, Prof. Dr. V. M. Avery, Assoc. Prof. Dr. K. T. Andrews[+]*
Eskitis Institute for Drug Discovery
Griffith University, QLD 4111 (Australia)
E-mail: k.andrews@griffith.edu.au

[c] *Dr. J. Held*
Institut für Tropenmedizin
Eberhard-Karls-Universität Tübingen, 72074 Tübingen (Germany)

[+] *K.T.A. and T.K. contributed equally to this work as senior authors.*

Histone deacetylase (HDAC) inhibitors are an emerging class of antiparasitic compounds.[8,9] HDACs play a key role in the epigenetic modulation of gene expression by altering chromatin structure,[10] and HDAC inhibitors have been widely studied and developed as effective treatments for human cancers.[8] HDAC gene homologues have been discovered in all *Plasmodium* species that can infect humans, and five HDAC-encoding genes have been identified in the *P. falciparum* genome.[11] Three of these *Pf*HDACs show homology to human class I (*Pf*HDAC1) or class II HDACs (*Pf*HDAC2,3), whereas two genes are class III homologues (*Pf*Sir2A and B).[8] The enzyme *P. falciparum* histone deacetylase 1 (*Pf*HDAC1) is considered an emerging target for malaria intervention strategies.[12] The potential of HDAC inhibitors for treating parasitic diseases was first reported in 1996 when the cyclic tetrapeptide apicidin was discovered to have broad-spectrum antiprotozoal activity.[13] Apicidin was also parenterally and orally active in vivo against *P. berghei* malaria in mice.[13] However, apicidin shows high toxicity towards normal mammalian cells and poor parasite selectivity (Selectivity Index (SI): 0.2–0.5).[8] Pan-inhibitors of human HDACs, such as vorinostat (SAHA) and trichostatin A (TSA), have potent antimalarial activity in vitro (Figure 1). These compounds cause hyperacetylation of *P. falciparum* histones, indicating inhibition of one or more *Pf*HDAC enzymes. TSA suffers from metabolic instability, but it has been considerably useful in helping our understanding of how HDAC inhibition affects malarial parasite growth, development, and transcriptional control.[8,14] WR301801 and SB939 (Figure 1) are two of the most promising antimalarial HDAC inhibitors studied to date, particularly in terms of in vivo efficacy in mouse malaria

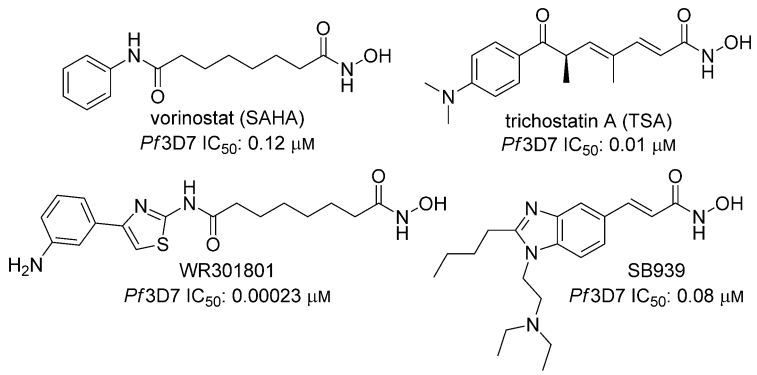

Figure 1. Selected antimalarial HDAC inhibitors. *Pf*3D7 data from references [9] (TSA), [16] (WR301801), and [17] (SAHA, SB939).

models. WR301801, identified by screening a panel of 50 phenylthiazolylhydroxamate-based HDAC inhibitors,[15] was able to cure mice when administered by intraperitoneal injection.[16] SB939 has also demonstrated in vivo efficacy in a murine model of cerebral malaria when administered orally to *P. berghei* ANKA-infected mice, preventing the development of cerebral malaria-like symptoms.[17] These data underscore the potential of HDAC inhibitors as novel leads for malaria drug research.

Structurally, HDAC inhibitors are characterized by a widely accepted pharmacophore model. Most HDAC inhibitors contain a cap group, a connecting-unit linker region, as well as a zinc binding group (ZBG).[18] The design of antimalarial HDAC inhibitors is challenging because of the lack of recombinant *Pf*HDAC2 and 3 enzymes and *Pf*HDAC crystal structures. It is therefore particularly important to develop comprehensive structure–activity relationships (SARs). The vast majority of antimalarial HDAC inhibitors contain hydroxamic acids as ZBGs, and only limited data are available regarding the antiplasmodial activity of HDAC inhibitors with alternative ZBGs.

In a previous study we discovered the promising anticancer activity of a new class of human HDAC inhibitors containing a novel alkoxyurea connection-unit linker region.[19] In this work, we explore the antimalarial properties of a panel of alkoxyurea-based HDAC inhibitors containing various cap groups and ZBGs. This allowed us to identify a number of notable SARs to establish design principles for the development of potent antimalarial HDAC inhibitors. All compounds were evaluated for in vitro activity against asexual blood-stage *P. falciparum* parasites. Representative compounds were then screened for gametocytocidal properties. In addition, selected compounds were examined for their cytotoxicity against a normal mammalian cell line and their ability to hyperacetylate histones in asexual-stage *P. falciparum* parasites as a marker of HDAC inhibition.

Results and Discussion

Synthesis

HDAC inhibitors **1e–l** and **2–5** were synthesized as described previously.[19] The novel alkoxyurea-based compounds **1a–d** were prepared from the readily available starting material **6** using an optimized synthetic protocol. Briefly, deprotection of the phthaloyl group was accomplished by treatment of **6** with methylhydrazine to furnish the aminoxy intermediate **7**. The respective aniline derivatives were activated with 1,1′-carbonyldiimidazole (CDI), and the resulting imidazolides were subsequently treated with **7** to provide the protected alkoxyureas **8a–d**. Finally, the *O*-benzyl protecting groups were cleaved by catalytic hydrogenation to afford HDAC inhibitors **1a–d** (Scheme 1).

In vitro activity against asexual-stage and gametocyte-stage parasites

The antimalarial activity of HDAC inhibitors **1a–l** and **2–5** was first tested against the chloroquine-sensitive

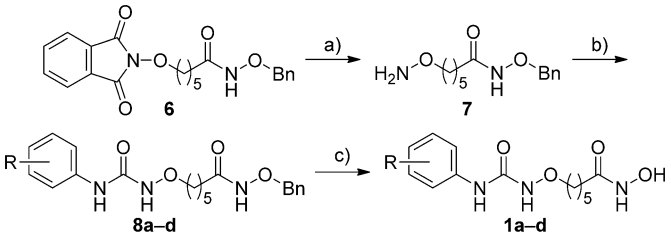

Scheme 1. Synthesis of alkoxyurea-based HDAC inhibitors **1a–d**. *Reagents and conditions*: a) methylhydrazine, CH_2Cl_2, −10 °C, 2 h, 57%; b) 1. aniline derivative, CDI, CH_2Cl_2, RT, 2 h, 2. **7**, Et_3N, RT, 18 h, 23–70%; c) Pd/C, H_2 (1 bar), THF, RT, 2 h, 41–83%.

3D7 line of *P. falciparum* using a [^{3}H]hypoxanthine incorporation assay. The calculated physicochemical properties of our alkoxyurea-based HDAC inhibitors indicates that all compounds comply with Lipinski's rules ($\log P < 5$, HBA < 10, HBD < 5, $M_r <$ 500 Da).[20] All compounds had calculated $\log P$ values between 0.49 and 2.85 (Table 1) and were thus expected to be cell permeable. When we examined the activity of alkoxyurea-based HDAC inhibitors against asexual blood-stage parasites, we found that 10 of 16 compounds tested (**1a**,**b** and **1d–k**) had IC_{50} values ≤ 1 μM, three had less potent activity with IC_{50} values between 1.4 and 2.6 μM (**1c**, **1l**, and **2**), while three (**3–5**) were inactive ($IC_{50} > 5$ μM, Table 1). These data provided a number of valuable SARs. In particular, all compounds with a classical hydroxamic acid as ZGB were active, whereas all compounds with alternative ZBGs were inactive. The data for the *N*-methylhydroxamic acid **3**, *o*-hydroxyanilide **4**, and *o*-aminoanilide **5** suggest that an unsubstituted hydroxamic acid group is crucial for potent activity against asexual blood-stage parasites. The chain-shortened derivative **2** ($n = 4$) displayed only moderate activity against the 3D7 line (IC_{50}: 1.86 μM), demonstrating that an elongated linker is required to efficiently access the active site zinc ion. All HDAC inhibitors of type **1** ($n = 5$), except compounds **1c** (R = PhO) and **1l** (R = 2-CH_3), were active against asexual blood-stage parasites at nanomolar concentrations. Five compounds (**1a**, **1e–h**) revealed potent

Table 1. Calculated log *P* values of alkoxyurea-based HDAC inhibitors and the in vitro activity against asexual blood stages of *P. falciparum* 3D7 and gametocyte stage parasites.

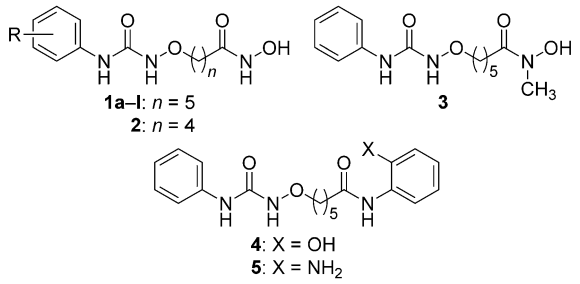

Compd	R	log *P*[a]	IC_{50} [μM] *Pf*3D7[b]	*Pf*LSG[c]
1a	4-PrO	1.56 ± 0.55	0.36 ± 0.05	5.49 ± 0.38
1b	4-C_2H_5O	1.02 ± 0.55	0.69 ± 0.17	ND
1c	4-PhO	2.57 ± 0.59	1.41 ± 0.19	ND
1d	4-Ph	2.61 ± 0.56	0.90 ± 0.12	1.71 ± 0.34
1e	4-*t*Bu	2.23 ± 0.54	0.16 ± 0.03	3.45 ± 0.76
1f	4-*i*Pr	1.88 ± 0.54	0.34 ± 0.06	ND
1g	4-CH_3	1.00 ± 0.54	0.44 ± 0.08	ND
1h	4-CH_3O	0.49 ± 0.55	0.48 ± 1.12	ND
1i	3,5-CH_3	1.46 ± 0.54	0.73 ± 0.06	3.33 ± 0.34
1j	3-CH_3	1.00 ± 0.54	0.74 ± 0.09	ND
1k	4-F	0.78 ± 0.02	0.78 ± 0.02	ND
1l	2-CH_3	1.00 ± 0.54	2.59 ± 0.62	ND
2	H	0.32 ± 0.54	1.86 ± 0.16	ND
3		1.24 ± 0.61	> 5	ND
4		2.85 ± 0.55	> 5	ND
5		2.26 ± 0.55	> 5	ND
chloroquine			0.006 ± 0.002	ND
SAHA			0.13 ± 0.02	ND
methylene blue			ND	0.23 ± 0.015
pyrimethamine			ND	> 120
artesunate			ND	0.0023 ± 0.0009

[a] log *P* values were calculated using ACD/ChemSketch freeware version 12.01. [b] *P. falciparum* 3D7 asexual-stage assays, $n = 3$, each in triplicate wells. [c] *P. falciparum* NF54 late-stage gametocytes (IV–V), $n = 2$, each in duplicate wells. ND: not determined.

activity with IC_{50} values ≤ 0.5 μM (Table 1). Interestingly, a bulky alkyl group at the 4-position emerged as being beneficial to activity, as indicated by the potent activity of compounds **1e** and **1f** (Table 1). Notably, compound **1e**, bearing a *tert*-butyl group at the 4-position, was the most active compound in this series (IC_{50}: 0.16 μM). The activity of **1e** against the 3D7 line of *P. falciparum* is similar to the activity of the reference compound SAHA (IC_{50}: 0.13 μM, Table 1).

The focus in malaria drug discovery is moving from prevention and treatment towards eradication. It is therefore of particular importance to identify new antimalarial agents with activity against sexual (gametocyte) stages and the ability to block the transmission to the mosquito vector. Thus, four structurally diverse HDAC inhibitors of type **1** were screened for activity against late-stage (IV–V) gametocytes using an imaging viability assay. All compounds (**1a**, **1d**, **1e**, and **1i**) showed moderate activity against late-stage gametocytes (IC_{50}: 1.71–5.49 μM, Table 1). Compound **1d**, bearing a biphenyl cap group revealed the highest activity (IC_{50}: 1.71 μM), which indicates that **1d** might be a suitable starting point for further drug design to develop alkoxyurea-based HDAC inhibitors with improved gametocytocidal properties.

Cytotoxicity and selectivity indices

To assess the selectivity of alkoxyurea-based HDAC inhibitors for *P. falciparum* parasites, the cytotoxicity of five representative compounds was determined with a normal human cell line (neonatal foreskin fibroblast (NFF) cells). As shown in Table 2, asexual-stage SIs ranged from 9 to 33, with the highest parasite-specific selectivity observed for **1a** and **1e** (SI: 33 and 31, respectively). Accordingly, the SIs of **1a** and **1e** are similar to those previously reported for SB939 and SAHA (SB939 $SI_{NFF/Pf3D7}$: 19, SAHA $SI_{NFF/Pf3D7}$: 41; Table 2). Compound **1e** is also the most potent against asexual-stage 3D7 parasites. In contrast to the asexual-stage data, the gametocyte selectivity of the alkoxyurea-based HDAC inhibitors was poor, with all compounds having $SI \leq 5$.

Table 2. Cytotoxicity and selectivity indices.

Compd	R	IC_{50} [μM][a]	SI[b] Asexual stage	Gametocyte
1a	4-PrO	11.9 ± 3.2	33	2
1d	4-Ph	7.9 ± 1.3	9	5
1e	4-*t*Bu	4.9 ± 2.0	31	2
1f	4-*i*Pr	7.6 ± 1.1	22	ND
1i	3,5-CH_3	7.7 ± 1.9	10	2
SAHA		4.9 ± 1.2[c]	41[c]	ND
SB939		1.5 ± 0.6[c]	19[c]	ND

[a] NFF cell line, data are the mean ± SD for $n = 3$ experiments. [b] SI = (mammalian cell IC_{50})/(*P. falciparum* IC_{50} (Table 1)); larger values indicate greater malaria parasite selectivity. [c] Data from reference [17]. ND: not determined.

Mode of action studies

The mode of action of five representative alkoxyurea-based HDAC inhibitors in asexual-stage parasites was determined by using an in situ histone hyperacetylation assay. Trophozoite-stage *P. falciparum* 3D7 parasites were incubated with $3 \times IC_{50}$ concentrations of **1a**, **1d**–**f**, or **1i**, or control compounds chloroquine (CQ) or SAHA. Following 3 h exposure, protein lysates were prepared and analyzed by western blot using antisera specific to anti-(tetra)acetyl histone H4. In comparison with vehicle controls (Figure 2; C-0h and C-3h) the control HDAC inhibitor SAHA, but not the antimalarial drug CQ, caused hyperacetylation of histone H4. Likewise, all five alkoxyurea-based HDAC inhibitors caused hyperacetylation of histone H4, confirming a mode of action against HDAC activity. Equivalent loading was confirmed by probing the same membrane with antisera that recognizes *P. falciparum* RAP2.

Conclusions

In summary, 16 HDAC inhibitors containing an alkoxyurea connecting-unit linker region were evaluated in vitro against the *P. falciparum* 3D7 line. From the data obtained, some SARs can

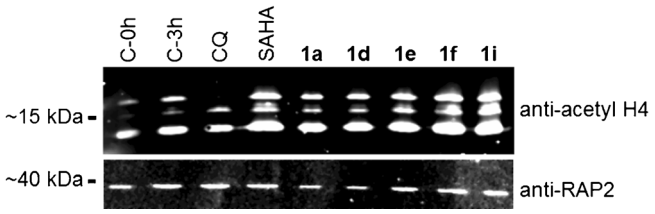

Figure 2. Hyperacetylation of *P. falciparum* histone H4 by alkoxyurea-based HDAC inhibitors. Trophozoite-stage *P. falciparum* 3D7 parasites were treated for 3 h with $3\times IC_{50}$ concentrations of chloroquine (CQ), SAHA, or the alkoxyurea-based HDAC inhibitors **1a**, **1d**, **1e**, **1f**, or **1i**. Protein lysates were analyzed by SDS-PAGE and western blot using antisera that recognizes acetylated forms of histone H4 (anti-(tetra)acetyl H4 (lysine 5, 8, 12, 16)). Antisera recognizing *Pf*RAP2 was used to assess loading.

be drawn: 1) a hydroxamic acid ZBG is crucial for antiplasmodial activity, 2) linker length appears to be critical for activity, and 3) bulky alkyl substituents at the 4-position of the cap group improve potency. When screened in vitro for their activity against sexual-stage *P. falciparum* parasites (stage IV–V gametocytes), compounds **1a**, **1d**, **1e**, and **1i** showed moderate gametocytocidal properties (IC_{50}: 1.71–5.49 μM). Selected compounds were shown to cause hyperacetylation of *P. falciparum* histone H4, and the most potent asexual stage inhibitor **1e** (*Pf*3D7 IC_{50}: 0.16 μM) was >30-fold more cytotoxic against the *P. falciparum* 3D7 line compared to normal mammalian cells. Thus, compound **1e** will serve as a starting point for future work to develop alkoxyurea-based HDAC inhibitors with enhanced parasite selectivity and improved antiplasmodial properties.

Experimental Section

Synthesis

All solvents and chemicals were used as purchased without further purification. The progress of all reactions was monitored on Merck pre-coated silica gel plates (with fluorescence indicator UV254) using EtOAc/*n*-hexane as solvent system. Column chromatography was performed with Macherey–Nagel silica gel 60M (0.04–0.063 mm) with the solvent mixtures specified in the corresponding experiment. Spots were visualized by irradiation with ultraviolet light (254 nm). Melting points (mp) were taken in open capillaries on a Mettler FP 5 melting-point apparatus and are uncorrected. Proton (^1H) and carbon (^{13}C) NMR spectra were recorded on a Bruker Avance 500 (500.13 MHz for ^1H, 125.76 MHz for ^{13}C) using [D_6]DMSO as solvent. Chemical shifts are given in parts per million (ppm), (δ relative to residual solvent peak for ^1H and ^{13}C or to tetramethylsilane). Elemental analysis was performed on a PerkinElmer PE 2400 CHN elemental analyzer. HPLC purity determination was carried out using a Phenomenex Luna C-18(2) 1.8 μm particle (250 mm × 4.6 mm) column, supported by Phenomenex Security Guard Cartridge Kit C_{18} (4.0 mm × 3.0 mm), isocratic (eluent: H_2O/CH_3CN 15:85 (*v*/*v*) containing 0.05% TFA) over 20 min at a flow rate of 0.8 mL min^{-1}. The purity of all final compounds was 98% or higher. HRMS analysis was performed on a UHR-TOF maXis 4G, Bruker Daltonics, Bremen (Germany). The synthesis of compounds **1e–l**, **2–5**, and **6** was described previously by us.[19]

Synthesis of 6-(aminooxy)-*N*-(benzyloxy)hexanamide (7): Methylhydrazine (1.68 mL, 32 mmol) was added dropwise at −10 °C to a solution of compound **6** (7.65 g, 20 mmol) in dry CH_2Cl_2 (50 mL). The reaction mixture was stirred for 2 h, and the precipitate was removed by filtration. The filtrate was evaporated under reduced pressure and treated with Et_2O (5 mL). The precipitate was removed by filtration, and a saturated solution of HCl in Et_2O was added to the filtrate to obtain the hydrochloride of the product. The solid was collected by filtration and subsequently dissolved in H_2O (15 mL). A saturated Na_2CO_3 solution was added until pH > 8, and the aqueous layer was extracted with EtOAc (3 × 30 mL). The combined organic layers were dried over Na_2SO_4 and evaporated under reduced pressure to provide **7** as a white solid (2.88 g, 57%): mp: 105 °C; ^1H NMR (500.13 MHz, [D_6]DMSO): δ = 10.94 (s, 1H), 7.42–7.27 (m, 5H), 5.86 (s, 2H), 4.77 (s, 2H), 3.48 (t, *J* = 6.5 Hz, 2H), 1.94 (t, *J* = 7.2 Hz, 2H), 1.50–1.35 (m, 4H), 1.30–1.20 ppm (m, 2H); ^{13}C NMR (125.76 MHz, [D_6]DMSO): δ = 169.20, 136.00, 128.65, 128.18, 128.09, 76.63, 74.61, 32.10, 27.59, 25.04, 24.75 ppm; Anal. calcd for $C_{13}H_{20}N_2O_3$: C 61.88, H 7.99, N 11.10, found: C 61.82, H 7.81, N 10.83.

General procedure for the preparation of *O*-benzyl-protected derivatives 8a–d: A solution of the respective aniline derivative (2 mmol) in dry CH_2Cl_2 (4 mL) was added dropwise to a suspension of CDI (0.357 g, 2.2 mmol) in dry CH_2Cl_2 (10 mL). The reaction mixture was stirred for 2 h at room temperature. Afterwards, 6-(aminooxy)-*N*-(benzyloxy)hexanamide (**7**) (0.505 g, 2 mmol) was added, and the reaction mixture was stirred overnight and subsequently evaporated under reduced pressure. The residue was dissolved in EtOAc (30 mL), and the solution was extracted with a saturated solution of $NaHCO_3$ (3 × 10 mL), H_2O (10 mL), 1 M HCl (10 mL), H_2O (10 mL), dried over Na_2SO_4, and evaporated under reduced pressure. The residue was purified by column chromatography using hexane/EtOAc (gradient 50:50 → 0:100) as eluent to afford compounds **8a–d**.

***N*-(Benzyloxy)-6-((3-(4-propoxyphenyl)ureido)oxy)hexanamide 8a**: white solid (0.198 g, 23%): mp: 101 °C; ^1H NMR (500.13 MHz, [D_6]DMSO): δ = 10.96 (s, 1H), 9.31 (s, 1H), 8.53 (s, 1H), 7.49–7.28 (m, 7H), 6.89–6.77 (m, 2H), 4.78 (s, 2H), 3.86 (t, *J* = 6.5 Hz, 2H), 3.73 (t, *J* = 6.7 Hz, 2H), 1.97 (t, *J* = 7.3 Hz, 2H), 1.76–1.66 (m, 2H), 1.65–1.56 (m, 2H), 1.56–1.46 (m, 2H), 1.35–1.24 (m, 2H), 0.96 ppm (t, *J* = 7.4 Hz, 3H); ^{13}C NMR (125.76 MHz, [D_6]DMSO): δ = 169.17, 157.25, 154.18, 135.98, 131.72, 128.65, 128.17, 128.08, 121.32, 114.09, 76.64, 75.47, 68.92, 32.05, 27.13, 24.70, 24.64, 21.99, 10.32 ppm; Anal. calcd for $C_{23}H_{31}N_3O_5$: C 64.32, H 7.27, N 9.78, found: C 64.34, H 7.20, N 9.66.

***N*-(Benzyloxy)-6-((3-(4-ethoxyphenyl)ureido)oxy)hexanamide 8b**: white solid (0.382 g, 46%): mp: 95 °C; ^1H NMR (500.13 MHz, [D_6]DMSO): δ = 10.95 (s, 1H), 9.31 (s, 1H), 8.52 (s, 1H), 7.53–7.30 (m, 7H), 6.82 (d, *J* = 8.9 Hz, 2H), 4.78 (s, 2H), 3.96 (q, *J* = 6.9 Hz, 2H), 3.74 (t, *J* = 6.8 Hz, 2H), 1.97 (t, *J* = 7.4 Hz, 2H), 1.68–1.57 (m, 2H), 1.56–1.46 (m, 2H), 1.37–1.22 ppm (m, 5H); ^{13}C NMR (125.76 MHz, [D_6]DMSO): δ = 169.19, 157.26, 154.04, 136.00, 131.72, 128.65, 128.17, 128.09, 121.35, 114.06, 76.65, 75.48, 62.94, 32.06, 27.13, 24.71, 24.64, 14.61 ppm; Anal. calcd for $C_{22}H_{29}N_3O_5$: C 63.60, H 7.04, N 10.11, found: C 63.88, H 7.02, N 9.82.

***N*-(Benzyloxy)-6-((3-(4-phenoxyphenyl)ureido)oxy)hexanamide 8c**: white solid (0.442 g, 53%): mp: 109 °C; ^1H NMR (500.13 MHz, [D_6]DMSO): δ = 10.96 (s, 1H), 9.44 (s, 1H), 8.73 (s, 1H), 7.64–7.53 (m, 2H), 7.44–7.30 (m, 7H), 7.15–7.03 (m, 1H), 7.00–6.88 (m, 4H), 4.78 (s, 2H), 3.75 (t, *J* = 6.7 Hz, 2H), 1.97 (t, *J* = 7.3 Hz, 2H), 1.67–1.57 (m, 2H), 1.57–1.47 (m, 2H), 1.38–1.25 ppm (m, 2H); ^{13}C NMR (125.76 MHz, [D_6]DMSO): δ = 169.17, 157.47, 157.09, 151.01, 135.98, 134.88, 129.80, 128.65, 128.16, 128.08, 122.66, 121.24, 119.26,

117.52, 76.63, 75.54, 32.05, 27.11, 24.69, 24.63 ppm; Anal. calcd for $C_{26}H_{29}N_3O_5$: C 67.37, H 6.31, N 9.07, found: C 67.10, H 6.42, N 9.18.

6-((3-([1,1′-Biphenyl]-4-yl)ureido)oxy)-*N*-(benzyloxy)hexanamide 8d: yellow solid (0.627 g, 70%): mp: 148 °C; ^{1}H NMR (500.13 MHz, [D$_6$]DMSO): δ = 10.98 (s, 1H), 9.50 (s, 1H), 8.80 (s, 1H), 7.71–7.66 (m, 2H), 7.64 (d, J = 7.5 Hz, 2H), 7.61–7.56 (m, 2H), 7.50–7.28 (m, 8H), 4.79 (s, 2H), 3.78 (t, J = 6.7 Hz, 2H), 1.98 (t, J = 7.1 Hz, 2H), 1.70–1.58 (m, 2H), 1.58–1.48 (m, 2H), 1.38–1.25 ppm (m, 2H); ^{13}C NMR (125.76 MHz, [D$_6$]DMSO): δ = 169.66, 157.42, 140.19, 138.96, 136.45, 134.46, 129.22, 129.13, 128.65, 128.56, 127.22, 127.03, 126.53, 120.17, 77.12, 76.06, 32.54, 27.60, 25.19, 25.12 ppm; Anal. calcd for $C_{26}H_{29}N_3O_4$: C 69.78, H 6.53, N 9.39, found: C 69.54, H 6.37, N 9.11.

General procedure for the preparation of HDAC inhibitors 1a–d: A solution of the respective *O*-benzyl-protected hydroxamic acid **8a–d** (0.5 mmol) in dry THF (50 mL) was hydrogenated (1 bar) at room temperature in the presence of a catalytic amount of Pd/C (10 wt%). Upon completion, the crude mixture was filtered through Celite to remove the catalyst, and the filtrate was concentrated under reduced pressure. The residue was purified by column chromatography using EtOAc or EtOAc/MeOH (9:1) as eluent.

***N*-Hydroxy-6-((3-(4-propoxyphenyl)ureido)oxy)hexanamide 1a**: beige solid (0.070 g, 41%): mp: 105 °C; ^{1}H NMR (500.13 MHz, [D$_6$]DMSO): δ = 10.36 (s, 1H), 9.31 (s, 1H), 8.69 (s, 1H), 8.53 (s, 1H), 7.46–7.38 (m, 2H), 6.88–6.80 (m, 2H), 3.87 (t, J = 6.6 Hz, 2H), 3.74 (t, J = 6.7 Hz, 2H), 1.96 (t, J = 7.4 Hz, 2H), 1.75–1.65 (m, 2H), 1.65–1.56 (m, 2H), 1.56–1.46 (m, 2H), 1.39–1.24 (m, 2H), 0.96 ppm (t, J = 7.4 Hz, 3H); ^{13}C NMR (125.76 MHz, [D$_6$]DMSO): δ = 169.42, 157.73, 154.66, 132.17, 121.82, 114.57, 75.97, 69.40, 32.56, 27.62, 25.30, 25.27, 22.45, 10.79 ppm; HRMS-ESI: m/z $[M+H]^+$ calcd for $C_{16}H_{26}N_3O_5$: 340.1867, found: 340.1865; Anal. calcd for $C_{16}H_{25}N_3O_5$: C 56.62, H 7.42, N 12.38, found: C 56.45, H 7.39, N 12.27.

6-((3-(4-Ethoxyphenyl)ureido)oxy)-*N*-hydroxyhexanamide 1b: white solid (0.073 g, 45%): mp: 93 °C; ^{1}H NMR (500.13 MHz, [D$_6$]DMSO): δ = 10.35 (s, 1H), 9.31 (s, 1H), 8.67 (s, 1H), 8.53 (s, 1H), 7.42 (d, J = 8.6 Hz, 2H), 6.83 (d, J = 8.6 Hz, 2H), 3.97 (q, J = 6.9 Hz, 2H), 3.74 (t, J = 6.7 Hz, 2H), 1.96 (t, J = 7.5 Hz, 2H), 1.68–1.57 (m, 2H), 1.56–1.47 (m, 2H), 1.39–1.25 ppm (m, 5H); ^{13}C NMR (125.76 MHz, [D$_6$]DMSO): δ = 168.93, 157.25, 154.03, 131.73, 121.35, 114.06, 75.51, 62.94, 32.09, 27.16, 24.84, 24.82, 14.61 ppm; HRMS-ESI: m/z $[M+H]^+$ calcd for $C_{15}H_{24}N_3O_5$: 326.1710, found: 326.1708; Anal. calcd for $C_{15}H_{23}N_3O_5$: C 55.37, H 7.13, N 12.91, found: C 55.12, H 7.00, N 12.72.

***N*-Hydroxy-6-((3-(4-phenoxyphenyl)ureido)oxy)hexanamide 1c**: grey solid (0.187 g, 63%): mp: 107 °C; ^{1}H NMR (500.13 MHz, [D$_6$]DMSO): δ = 10.36 (s, 1H), 9.44 (s, 1H), 8.74 (s, 1H), 8.68 (s, 1H), 7.64–7.52 (m, 2H), 7.40–7.32 (m, 2H), 7.09 (t, J = 7.4 Hz, 1H), 7.00–6.88 (m, 4H), 3.75 (t, J = 6.7 Hz, 2H), 1.96 (t, J = 7.4 Hz, 2H), 1.69–1.57 (m, 2H), 1.56–1.46 (m, 2H), 1.40–1.24 ppm (m, 2H); ^{13}C NMR (125.76 MHz, [D$_6$]DMSO): δ = 168.90, 157.47, 157.08, 151.01, 134.88, 129.80, 122.67, 121.25, 119.26, 117.52, 75.57, 32.09, 27.14, 24.82, 24.80 ppm; HRMS-ESI: m/z $[M+H]^+$ calcd for $C_{19}H_{24}N_3O_5$: 374.1710, found: 374.1712; Anal. calcd for $C_{19}H_{23}N_3O_5$: C 61.11, H 6.21, N 11.25, found: C 61.01, H 6.39, N 11.15.

6-((3-([1,1′-Biphenyl]-4-yl)ureido)oxy)-*N*-hydroxyhexanamide (1d): beige solid (0.148 g, 83%): mp: 141 °C; ^{1}H NMR (500.13 MHz, [D$_6$]DMSO): δ = 10.37 (s, 1H), 9.50 (s, 1H), 8.80 (s, 1H), 8.69 (s, 1H), 7.68 (d, J = 8.3 Hz, 2H), 7.64 (d, J = 7.7 Hz, 2H), 7.59 (d, J = 8.3 Hz, 2H), 7.44 (t, J = 7.6 Hz, 2H), 7.32 (t, J = 7.4 Hz, 1H), 3.78 (t, J = 6.7 Hz, 2H), 1.98 (t, J = 7.4 Hz, 2H), 1.71–1.60 (m, 2H), 1.58–1.47 (m, 2H), 1.43–1.26 ppm (m, 2H); ^{13}C NMR (125.76 MHz, [D$_6$]DMSO): δ = 169.39, 157.41, 140.20, 138.97, 134.46, 129.22, 127.22, 127.03, 126.53, 120.18, 76.09, 32.58, 27.63, 25.31, 25.30 ppm; HRMS-ESI: m/z $[M+H]^+$ calcd for $C_{19}H_{24}N_3O_4$: 358.1761, found: 358.1763. HPLC purity: 99.04%.

Biological assays

Asexual in vitro antimalarial assays: Asexual-stage growth inhibition assays were carried out using *P. falciparum* line 3D7 parasites and the [^{3}H]hypoxanthine incorporation method, essentially as previously described.[17,21] Test compounds diluted in parasite culture media (RPMI 1640 supplemented with 10% heat-inactivated human serum) were incubated with synchronous ring-stage parasites (0.25% parasitemia and 2.5% hematocrit) for 48 h at 37 °C under standard parasite culture conditions, followed by the addition of [^{3}H]hypoxanthine (0.5 μCi per well). After a further 24 h culture, [^{3}H]hypoxanthine incorporation was measured by harvesting onto 1450 MicroBeta filter mats (Wallac) and counting using a 1450 MicroBeta liquid scintillation counter. Percentage inhibition of growth relative to vehicle controls (0.5% DMSO) was determined for three independent experiments, carried out in triplicate wells. Chloroquine was included in each assay as a positive control. IC_{50} values were calculated using log–linear interpolation of inhibition curves[22] and are presented as mean ± SD for the three independent assays.

Late-stage P. falciparum (IV–V) anti-gametocyte assays: This assay was undertaken as described previously.[23] Briefly, highly synchronous stage IV gametocytes, induced from transgenic NF45 *P. falciparum* parasites expressing the gametocyte-specific protein *Pf*s16, fused to green fluorescent protein (NF-54-*Pf*s16-GFP), were isolated by magnetic column on day 8 post-induction. Gametocytes were added to 384-well imaging plates, containing test and control compounds, at 33000 gametocytes per well, and the plates were incubated for 72 h under reduced oxygen tension (5% CO_2, 5% O_2, 80% N_2). Mitotracker Red CM-H2XRos (0.07 μg mL^{-1}, 5 μL) was added to each well and incubated overnight as described above. Gametocyte viability was evaluated on an OPERA (PerkinElmer) High-Content Screening System. Images acquired for GFP and Mitotracker Red CM-H2XRos were overlaid, and the number of elongated viable gametocytes per image was determined using a script based on Acapella software, developed for use with the OPERA imaging system. Relative percent inhibition relative to 0.4% DMSO (vehicle control) and 5 μM puromycin was calculated, and the mean IC_{50} values ± SD were determined by four-parameter nonlinear regression analysis, sigmoidal dose–response (variable slope) fit using Prism 4.0 for two separate experiments in quadruplicate point.

Principle of script used for image analysis: Maximal fluorescent pixel intensities are identified for the MTR-acquired image, and the average intensity for designated objects calculated. Objects with an average fluorescent MTR intensity, above an assay-specified classification of minimal MTR signal, are identified as viable objects. GFP-positive objects are identified and overlaid with the MTR-positive objects. The GFP objects with an MTR-positive signal are then evaluated for the characteristic of being at least fourfold longer than they are wide. Objects that are both MTR-positive and GFP-object-elongated are identified as viable late-stage gametocytes.

In vitro mammalian cell toxicity assays: Cytotoxicity assays were carried out essentially as previously described.[24] Briefly, neonatal foreskin fibroblast (NFF) cells were cultured in RPMI media (Life Technologies) supplemented with 10% heat-inactivated fetal calf serum

(CSL Biosciences), and 1% penicillin–streptomycin (Life Technologies). Cells were seeded into wells of 96-well tissue culture plates (3000 cells per well), cultured for 24 h at 37 °C and 5% CO_2, then treated with a dilution series of each test or control compound. After 72 h, the medium was removed, plates were washed in PBS, and cells fixed with denatured alcohol. After washing with water, sulforhodamine B (50 μL, 0.4% in 1% acetic acid; Sigma) was added. Plates were incubated for 1 h prior to washing three times with 1% acetic acid. Each well then received 100 μL of 10 mM Tris base (unbuffered, pH > 9) prior to reading at 564 nm in an ELISA microplate reader. Percent growth inhibition relative to matched DMSO controls (0.5%) was then determined. Assays were carried out on three separate occasions, each with triplicate test wells. Chloroquine was included as an internal control in each assay. IC_{50} values were determined by log–linear interpolation of inhibition curves,[22] and are presented as mean ± SD of the three independent assays.

Histone hyperacetylation assays: The effect of compounds on histone acetylation was determined as previously described.[17] Briefly, trophozoite-stage *P. falciparum* 3D7 parasites were incubated for 3 h with $3 \times IC_{50}$ concentrations of the control HDAC inhibitor SAHA, the antimalarial drug chloroquine, or compounds **1a**, **1d**–**f**, or **1i**. Vehicle control (0.05% DMSO) samples were taken as the start ($t = 0$ h) and end ($t = 3$ h) of the treatment. Protein lysates were prepared and resuspended in SDS-PAGE loading dye before heat denaturing at 96 °C, then separating by 15% SDS-PAGE. Two-color western blot was carried out by using Odyssey reagents (LI-COR Biosciences) according to the manufacturers' instructions. The following primary antisera were used: anti-(tetra)acetyl H4 (Millipore) which recognizes lysines 5, 8, 12, and 16 of histone H4, and anti-IC3/94 monoclonal antisera which was used as a loading control and recognizes *P. falciparum* rhoptry-associated protein 2 (RAP2).[25] IRDye secondary antibodies (LI-COR Biosciences) were used, and membranes imaged using an Odyssey infrared imaging system (LI-COR biosciences).

Acknowledgements

The Deutsche Forschungsgemeinschaft (DFG) is acknowledged for funds used to purchase the UHR-TOF maXis 4G (Bruker Daltonics, Bremen) HRMS instrument used in this research. The Australian Research Council is acknowledged for research support (FT0991213 to K.T.A. and LP120200557 to V.M.A.). We thank the Australian Red Cross Blood Service for provision of human blood and sera.

Keywords: gametocytocides · histone deacetylases · inhibitors · malaria · *Plasmodium falciparum*

[1] World Health Organization, *World Malaria Report 2011*, WHO Press, Geneva, **2012**.
[2] S. Abdulla, N. Salim, F. Machera, R. Kamata, O. Juma, M. Shomari, S. Kubhoja, A. Mohammed, G. Mwangoka, T. Aebi, H. Mshinda, D. Schellenberg, T. Carter, T. Villafana, M.-C. Dubois, A. Leach, M. Lievens, J. Vekemans, J. Cohen, W. R. Ballou, M. Tanner, *Malar. J.* **2013**, *12*, 11.
[3] S. T. Agnandji, B. Lell, S. S. Soulanoudjingar, J. F. Fernandes, B. P. Abossolo, C. Conzelmann, B. G. Methogo, Y. Doucka, A. Flamen, B. Mordmüller, S. Issifou, P. G. Kremsner, J. Sacarlal, P. Aide, M. Lanaspa, J. J. Aponte, A. Nhamuave, D. Quelhas, Q. Bassat, S. Mandjate, E. Macete, P. Alonso, S. Abdulla, N. Salim, O. Juma, M. Shomari, K. Shubis, F. Machera, A. S. Hamad, R. Minja, A. Mtoro, A. Sykes, S. Ahmed, A. M. Urassa, A. M. Ali, G. Mwangoka, M. Tanner, H. Tinto, U. D'Alessandro, H. Sorgho, I. Valea, M. C. Tahita, W. Kabore, S. Ouedraogo, Y. Sandrine, R. T. Guiguemde, J. B. Ouedraogo, M. J. Hamel, S. Kariuki, C. Odero, M. Oneko, K. Otieno, N. Awino, J. Omoto, J. Williamson, V. Muturi-Kioi, K. F. Laserson, L. Slutsker, W. Otieno, L. Otieno, O. Nekoye, S. Gondi, A. Otieno, B. Ogutu, R. Wasuna, V. Owira, D. Jones, A. A. Onyango, P. Njuguna, R. Chilengi, P. Akoo, C. Kerubo, J. Gitaka, C. Maingi, T. Lang, A. Olotu, B. Tsofa, P. Bejon, N. Peshu, K. Marsh, S. Owusu-Agyei, K. P. Asante, K. Osei-Kwakye, O. Boahen, S. Ayamba, K. Kayan, R. Owusu-Ofori, D. Dosoo, I. Asante, G. Adjei, D. Chandramohan, B. Greenwood, J. Lusingu, S. Gesase, A. Malabeja, O. Abdul, H. Kilavo, C. Mahende, E. Liheluka, M. Lemnge, T. Theander, C. Drakeley, D. Ansong, T. Agbenyega, S. Adjei, H. O. Boateng, T. Rettig, J. Bawa, J. Sylverken, D. Sambian, A. Agyekum, L. Owusu, F. Martinson, I. Hoffman, T. Mvalo, P. Kamthunzi, R. Nkomo, A. Msika, A. Jumbe, N. Chome, D. Nyakuipa, J. Chintedza, W. R. Ballou, M. Bruls, J. Cohen, Y. Guerra, E. Jongert, D. Lapierre, A. Leach, M. Lievens, O. Ofori-Anyinam, J. Vekemans, T. Carter, D. Leboulleux, C. Loucq, A. Radford, B. Savarese, D. Schellenberg, M. Sillman, P. Vansadia, *N. Engl. J. Med.* **2011**, *365*, 1863–1875.
[4] S. Turschner, T. Efferth, *Mini-Rev. Med. Chem.* **2009**, *9*, 206–214.
[5] A. M. Dondorp, F. Nosten, P. Yi, D. Das, A. P. Phyo, J. Tarning, K. M. Lwin, F. Ariey, W. Hanpithakpong, S. J. Lee, P. Ringwald, K. Silamut, M. Imwong, K. Chotivanich, P. Lim, T. Herdman, S. S. An, S. Yeung, P. Singhasivanon, N. P. Day, N. Lindegardh, D. Socheat, N. J. White, *N. Engl. J. Med.* **2009**, *361*, 455–467.
[6] A. M. Dondorp, S. Yeung, L. White, C. Nguon, N. P. Day, D. Socheat, L. von Seidlein, *Nat. Rev. Microbiol.* **2010**, *8*, 272–280.
[7] WHO Global Plan for Artemisinin Resistance Containment (GPARC), World Health Organization, Geneva, **2011**.
[8] K. T. Andrews, T. N. Tran, D. P. Fairlie, *Curr. Pharm. Des.* **2012**, *18*, 3467–3479.
[9] K. T. Andrews, T. N. Tran, N. C. Wheatley, D. P. Fairlie, *Curr. Top. Med. Chem.* **2009**, *9*, 292–308.
[10] O. Witt, H. E. Deubzer, T. Milde, I. Oehme, *Cancer Lett.* **2009**, *277*, 8–21.
[11] P. Horrocks, E. Wong, K. Russell, R. D. Emes, *Mol. Biochem. Parasitol.* **2009**, *164*, 9–25.
[12] V. Patel, R. Mazitschek, B. Coleman, C. Nguyen, S. Urgaonkar, J. Cortese, R. H. Barker, E. Greenberg, W. Tang, J. E. Bradner, S. L. Schreiber, M. T. Duraisingh, D. F. Wirth, J. Clardy, *J. Med. Chem.* **2009**, *52*, 2185–2187.
[13] S. J. Darkin-Rattray, A. M. Gurnett, R. W. Myers, P. M. Dulski, T. M. Crumley, J. J. Allocco, C. Cannova, P. T. Meinke, S. L. Colletti, M. A. Bednarek, S. B. Singh, M. A. Goetz, A. W. Dombrowski, J. D. Polishook, D. M. Schmatz, *Proc. Natl. Acad. Sci. USA* **1996**, *93*, 13143–13147.
[14] K. T. Andrews, A. P. Gupta, T. N. Tran, D. P. Fairlie, G. N. Gobert, *PLoS One* **2012**, *7*, e31847.
[15] G. S. Dow, Y. Chen, K. T. Andrews, D. Caridha, L. Gerena, M. Gettayacamin, J. Johnson, Q. Li, V. Melendez, N. Obaldia, T. N. Tran, A. P. Kozikowski, *Antimicrob. Agents Chemother.* **2008**, *52*, 3467–3477.
[16] S. Agbor-Enoh, C. Seudieu, E. Davidson, A. Dritschilo, M. Jung, *Antimicrob. Agents Chemother.* **2009**, *53*, 1727–1734.
[17] S. D. M. Sumanadasa, C. D. Goodman, A. J. Lucke, T. Skinner-Adams, I. Sahama, A. Haque, T. A. Do, G. I. McFadden, D. P. Fairlie, K. T. Andrews, *Antimicrob. Agents Chemother.* **2012**, *56*, 3849–3856.
[18] P. Bertrand, *Eur. J. Med. Chem.* **2010**, *45*, 2095–2116.
[19] L. Marek, A. Hamacher, F. K. Hansen, K. Kuna, H. Gohlke, M. U. Kassack, T. Kurz, *J. Med. Chem.* **2013**, *56*, 427–436.
[20] C. A. Lipinski, F. Lombardo, B. W. Dominy, P. J. Feeney, *Adv. Drug Delivery Rev.* **2001**, *46*, 3–26.
[21] R. E. Desjardins, C. J. Canfield, J. D. Haynes, J. D. Chulay, *Antimicrob. Agents Chemother.* **1979**, *16*, 710–718.
[22] W. Huber, J. C. Koella, *Acta Trop.* **1993**, *55*, 257–261.
[23] S. Duffy, V. M. Avery, *Malar. J.* **2013**, *12*, 408.
[24] R. A. Davis, A. R. Carroll, K. T. Andrews, G. M. Boyle, T. L. Tran, P. C. Healy, J. A. Kalaitzis, R. G. Shivas, *Org. Biomol. Chem.* **2010**, *8*, 1785–1790.
[25] D. L. Baldi, K. T. Andrews, R. F. Waller, D. S. Roos, R. F. Howard, B. S. Crabb, A. F. Cowman, *EMBO J.* **2000**, *19*, 2435–2443.

Received: November 15, 2013
Revised: January 6, 2014
Published online on February 4, 2014